POROUS CHITOSAN MICROFILTRATION MEMBRANES FOR MICROPLASTICS REMOVAL

Mateusz Cegłowski[1,a], Monika Walczak[1,b], Maciej Szwast[2,c], Daniel Polak[2,d], Paweł Ruśkowski[1,e], Agnieszka Gadomska-Gajadhur[1,f,*]

[1] – Faculty of Chemistry, Warsaw University of Technology, Noakowskiego 3 Str., 00-664 Warsaw, Poland
[a] – ORCID: 0000-0002-8145-5271, [b] – ORCID: 0009-0009-6386-8900,
[e] – ORCID: 0000-0002-4589-0727, [f] – ORCID: 0000-0001-7686-1745
[2] – Faculty of Chemical and Process Engineering, Warsaw University of Technology, Waryńskiego 1 Str., 00-645 Warsaw, Poland
[c] – ORCID: 0000-0002-8414-7493, [d] – ORCID: 0000-0003-1658-3506
**corresponding author: agnieszka.gajadhur@pw.edu.pl*

Abstract

Microplastic contamination in water is a global problem, and its removal via membrane separation is considered one of the best solutions. Polymers traditionally used pose a threat if becoming the source of this exact pollutant. Chitosan was investigated for the production of microfiltration membranes potentially dedicated to water filtration in a dead-end regime. Two variants of phase inversion, coupled with neutralisation of the chitosan salt, were tested. Mechanical strength, surface wettability, morphology, and the separation efficiency of polyvinyl chloride microplastics were investigated. Membranes produced by precipitation from the concentrated solution proved to be suitable for the filtration application, contrary to those made as dried films produced with porogenic agents, with even >99% overall separation efficiency.

Keywords: *microfiltration, microplastics, water treatment, membranes*

Received: 12.03.2026
Accepted: 04.06.2026

1. Introduction

Microplastic pollution of the water environment has become a major problem in recent years. This poses a threat to the health of living organisms to an unknown extent. Most of these pollutants come from land-based sources, and around a quarter of them pass through wastewater treatment plants (WWTPs) [1]. Those facilities are crucial points at which microplastics can be captured and disintegrated by appropriate methods. Standard processes in WWTPs remove a significant portion of microplastics, but maximising their efficiency is particularly important from an ecotoxicological perspective [2, 3]. Membrane filtration presents itself as a cost-effective and efficient solution for tertiary treatment in WWTPs, capable of removing up to 100% of microplastics [4]. Nevertheless, most research does not consider the smallest particles, those under 1 μm [5]. The typical sizes of microparticles investigated are in the range of tens to hundreds of micrometres, for which there are many detection and quantification methods available. For such big particles, even the basic commercial membranes can be as efficient as those designed for this specific pollutant [6, 7].

In the context of microplastic pollution, typical membrane filtration has a specific problem that is not widely considered, which is the emission of microplastics by the membrane itself. Typically, filtration membranes are made from polyethersulfone, polyvinyl chloride (PVC), polypropylene, or polyvinylidene fluoride, and these polymers can be released as microparticles during operation [8]. Thus, the best solution is to use materials that will not become microplastics. According to European Union regulations, such material should be either soluble in water, biodegradable in a reasonable time, made without a carbon-based polymer, or chemically unmodified, natural polymer [9]. Chitosan is an abundant, biodegradable polymer and has already been used in water treatment for its excellent adsorptive properties [10, 11]. Despite its mechanical properties being poor without additional reinforcements or modifications [12], there are reports on the successful utilisation of chitosan in membrane processes [13–16].

The aim of this study is to develop and assess the efficiency of a microfiltration membrane for the separation of microplastics from water with a cut-off point below 1 μm using only eco-friendly and non-toxic resources.

2. Materials and Methods

2.1. Materials

Chitosan of low molecular weight (30–100 cps, ≥ 90.0% deacetylation, Pol-Aura, Poland), tannic acid (pure, Aktyn, Poland), anhydrous citric acid (CA, food grade, ≥ 99.5%, EcoFlores, Poland), polyethylene glycol 200 (PEG 200, Chemat, Poland), glucose (food grade, Delecta, Poland), potassium hydroxide (p.a., POCH, Poland), glycerol (pharmaceutical grade, ≥ 99.5%, Brenntag, Poland), Ludwik hypoallergenic dish soap (5–15% anionic surfactants, < 5% non-ionic surfactants, < 5% amphoteric surfactants, INCO group, Poland), PVC particles (Slovinyl® EP-702, < 63 μm, Chemox Holding s.r.o., Slovakia) were used as received, without further purification. Water was sourced from the Direct-Q® 3 UV purification system (Merck Millipore) unless stated otherwise. Control membranes (Durapore® 0.1 μm PVDF membrane, 47 mm, hydrophilic, nonsterile, Merck Millipore, Ireland) were used as received. The Slovinyl® EP-702 particle size distribution was measured by Static Light Scattering (SLS) with Malvern MasterSizer in isopropanol after ultrasonication (Figure 1).

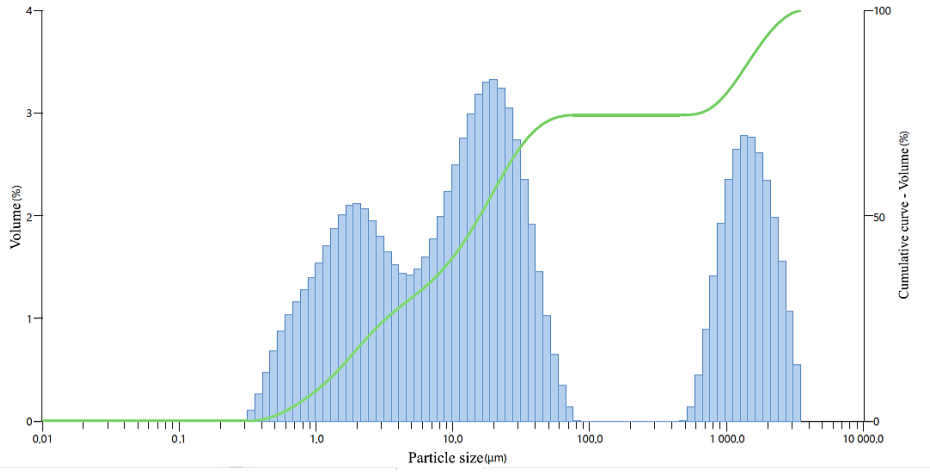

Figure 1. Size distribution of Slovinyl EP-702 PVC particles.

2.2. Membrane preparation

Uniform amounts of chitosan and tannic acid, as well as varied amounts of PEG, were weighed into a 100 mL container. 100 mL of a 4% CA solution was added to each composition, and the mixture was stirred with a magnetic stirrer in a closed container for at least 24 h until complete dissolution. Different masses of glucose were then added and stirred until complete dissolution. The variation in the PEG 200-to-glucose ratio was indicated on the sample labels as numbers (1, 2, and 3) (Table 1). Each sample was prepared in duplicate, denoted as 'a' or 'b' in sample names. The mixture was degassed under vacuum (50 mbar) for 30 min. The prepared solution was poured into a PTFE mould with internal dimensions of 200 mm × 200 mm × 2 mm. The solution did not pour completely over due to surface tension and poor wettability of the mould. The mould was placed in a laboratory oven (SLW 180 SMART, Pol-Eko Aparatura, Poland) at 60 °C for either 2 h (variant G, concentrated by evaporation) or 5.5 h (variant D, fully dried to form a solid state). After drying, the mould was moved into a ceramic container, 80 mL of 2.5M KOH solution was added, and the mould was covered with paper to reduce evaporation. After 20 h of storage at room temperature, the membrane was removed and placed in a 1.5 L water (room temperature) for the next 20 h. The washed membrane was briefly dried at room temperature, covered with glycerol for 5–10 min and, after removal of excess glycerol, stored at room temperature in an envelope made from filtration paper. A reference chitosan material (R) was prepared in the same manner in a mould of 200 mm × 100 mm × 2 mm dimensions. Compositions and drying parameters are presented in Table 1.

2.3. Surface Wettability and Surface Free Energy (SFE)

The wettability of the membranes was measured with water and diiodomethane using a goniometer of Delta Optics BioLight 200 optical microscope with ToupTek microQ UCMOS01300KPA digital camera. Samples were cut into fragments with 0.5 cm × 2 cm area using a scalpel and shaken in 50 mL of water in an orbital shaker overnight to remove free glycerol. Then the surface was dried, and samples were placed on a metal stage for analysis. The static contact angle was measured using the sessile drop method. At least 5 contact angles from at least 3 sitting drops were measured for each liquid on each membrane. Results were averaged, and SFE and its components were calculated

in accordance with the OWRK method presented in ISO 19403-2 standard. Uncertainties of SFE components were calculated based on the standard deviation of measured contact angles.

Table 1. Membrane compositions and drying parameters.

Label	Chitosan [g]	PEG 200 [g]	Glucose [g]	Tannic acid [g]	4% CA acid solution [mL]	Drying time [h]
R	1.3	-	-	0.05	45	5
G1a	2.6	1.3	1.3	0.1	100	2
G1b						
G2a		0.65	1.95			
G2b						
G3a		1.95	0.65			
G3b						
D1a	2.6	1.3	1.3	0.1		5.5
D1b						
D2a		0.65	1.95			
D2b						
D3a		1.95	0.65			
D3b						

2.4. Mechanical Testing

The tensile strength was measured with an Instron 3366 test frame with a 10 kN load cell at 20 °C. From each membrane, 3 bar specimens of 1 cm × 5 cm were cut. Each sample was measured with a calliper and subjected to tensile loading at a constant rate of 5 mm/min until failure. Young's modulus was calculated from the slope of the linear region of the stress-strain curve, obtained by linear regression of the measured data in the range 0.5–2.0 % of maximum elongation.

2.5. Membrane Surface Morphology

A Phenom-World Phenom G2 (Phenom-World BV, Netherlands) Scanning Electron Microscope (SEM) was used to analyse the morphology of the membrane surface. Samples of approximately 0.5 cm × 0.5 cm were mounted on a SEM table with carbon tape and analysed in backscattered electron detection mode (BSE).

2.6. Filtration Experiment

A Suspension of Slovinyl® EP-702 PVC was prepared by adding 11 mg of PVC particles to 2000 mL of water containing 1.52 g of hypoallergenic dish detergent as a surfactant. The suspension was thoroughly stirred with a magnetic stirrer for 7 days in a closed glass flask.

From each membrane, a 50-mm-diameter circle was cut and placed on a metal net support in a membrane module (active surface area of 12.57 cm^2) with bypass, equipped with a peristaltic pump (Elpin+ 372A, Elpin+, Poland) and a manometer, as presented in Figure 2.

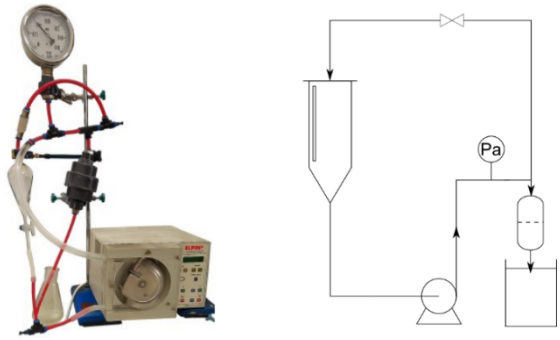

Figure 2. A photo and a technical scheme of the membrane module set-up.

For each membrane and an empty module as a reference, ca. 100 g of the PVC suspension was used as the feed. The 1.8–2 bar transmembrane pressure was kept constant over the filtration process. If no permeate was detected after 15 min of operation, the experiment was terminated and the membrane was described as non-permeable. Otherwise, at least 200 mL of water was fed through the pump afterwards to wash away the PVC residue, and the wash was collected alongside the filtered suspension in a glass flask to ensure complete transfer of the suspension through the membrane.

Collected filtrates were then filtered through a Durapore 0.1 µm PVDF membrane mounted in a glass vacuum membrane module, and everything was thoroughly washed with water to recover all PVC particles. PVDF membranes with PVC were then covered and dried at room temperature. From each PVDF membrane, a sample of approximately 0.5 cm × 0.5 cm was cut, mounted on a SEM table with the active surface upward, then analysed in BSE mode with Phenom G2 SEM. At least 3 images of 100 µm × 100 µm dimensions were collected from random visualised sample areas. Those images were then analysed by manually counting and measuring PVC microparticles with ToupTek ToupView 4.12 software. Measured particles were grouped into size classes with a width of 0.1 µm, and the filtration efficiency was then calculated and compared to the reference sample for each tested membrane.

3. Results and Discussion

3.1. Membranes Characterisation

The overall procedure for membrane fabrication presented in this research is well established [14], but the specifics differ. Based on the literature, the use of citric acid (CA) instead of the typical acetic acid was proposed, due to the possible crosslinking of chitosan by CA through amidation or hydrogen bonding [17–19]. The role of applied tannic acid was to form hydrogen bonds with chitosan and its crosslinking [20, 21], as well as increasing the hydrophilicity of the membrane, while the glucose and PEG 200 acted as porogens. The neutralisation step with a strong base was included to transform chitosan citrate back into chitosan, making the membrane insoluble in water. The drawback of the proposed preparation procedure is the need for membrane water storage or its plasticisation, e.g., with glycerol. Otherwise, the dry material becomes brittle and cannot be restored to its original state.

During neutralisation, variants D exhibited a slight shrinkage of below 5%, which was not observed in variants G. The second variable, the ratio of PEG 200 to glucose, did not result in visible variation between membranes. The SEM images of the upper surface of the produced membranes are shown in Figure 3.

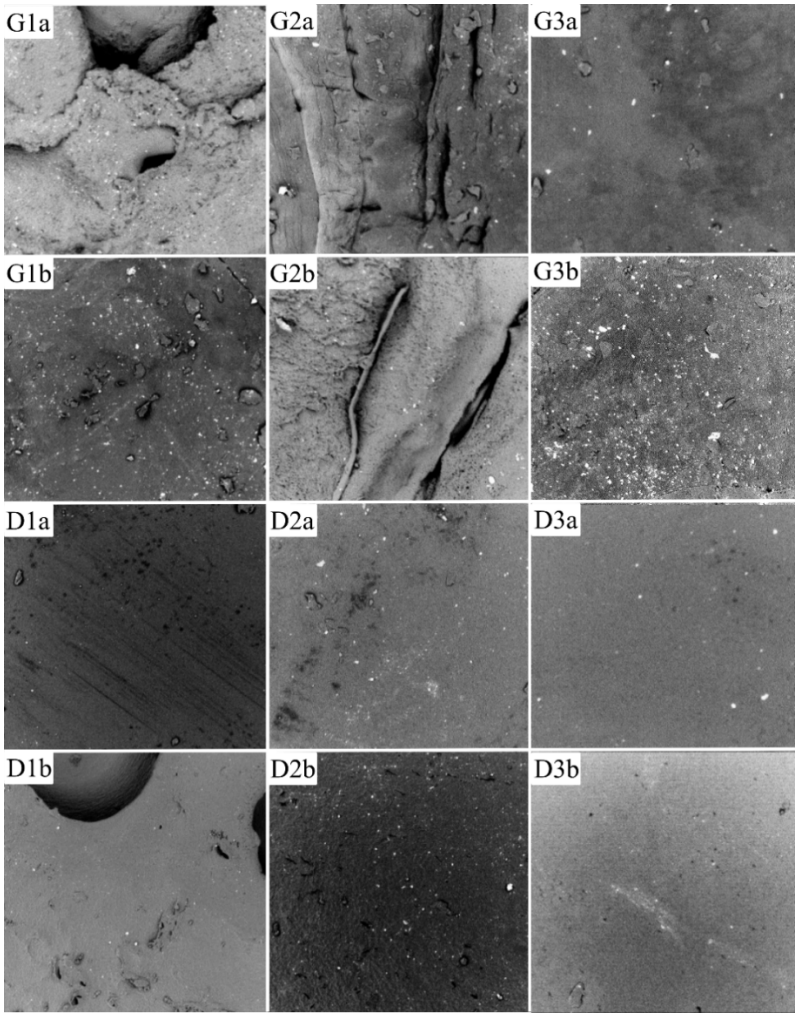

Figure 3. SEM images of the membrane's surface at 500× magnification.

The membranes' surfaces were unstable during SEM analysis. At high magnification, the pore opening was observed, and the surface visibly sank under an applied electron beam. Such deformations indicate that the structure of the membrane is not rigid. The D1-D3 membranes exhibit a much flatter and more regular surface morphology than G1-G3. The surface morphology of G1-G3 membranes results from treatment with a KOH solution, producing both irregular shapes and flat surfaces, depending on local turbulence and precipitation rate. As the surface of the D series membranes was solid when treated with KOH solution, the morphology results solely from the drying step. Additionally, within each D and G series, all membranes with higher PEG content exhibit flatter surfaces with very few visible pores. In turn, the most porous surface characteristics were observed for membranes with equal PEG and glucose contents (1.3 g each). Comparing the edges of both D and G materials (Figure 4), both types exhibit a porous internal structure, with the dried membrane having numerous smaller pores.

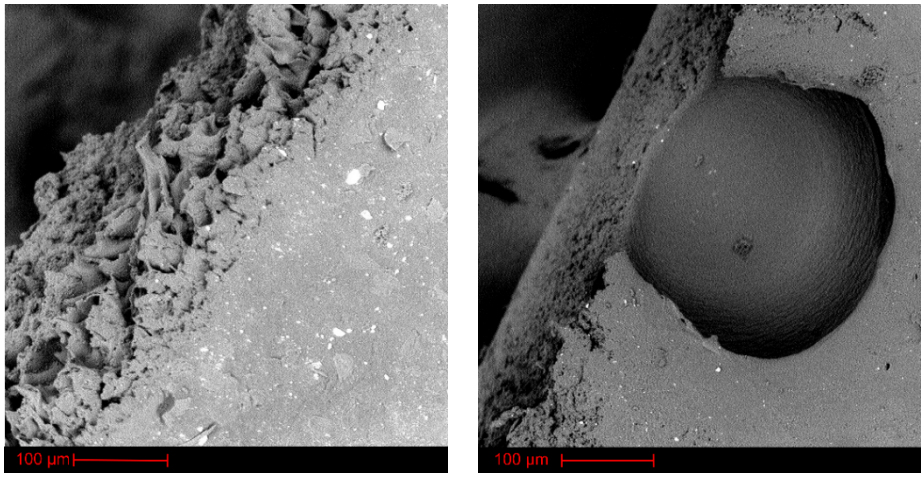

Figure 4. Edge of (a) G3b and (b) D2b membranes.

Both the D and G series exhibited a hydrophilic surface nature. Water contact angles for D series was 52–73 °, while 31–58 ° was found for G series, and 73–76 ° for pure chitosan membrane. The calculated polar and dispersive SFE components (Figure 5) also show the difference between D and G membranes' surfaces with generally similar dispersive components, but higher polar components of the latter. Compared to the pure chitosan membrane, the applied additives (tannic acid, PEG 200, glucose) caused only a slight increase in polar components in D1-D3 membranes, but a more than 2-fold increase in G1-G3.

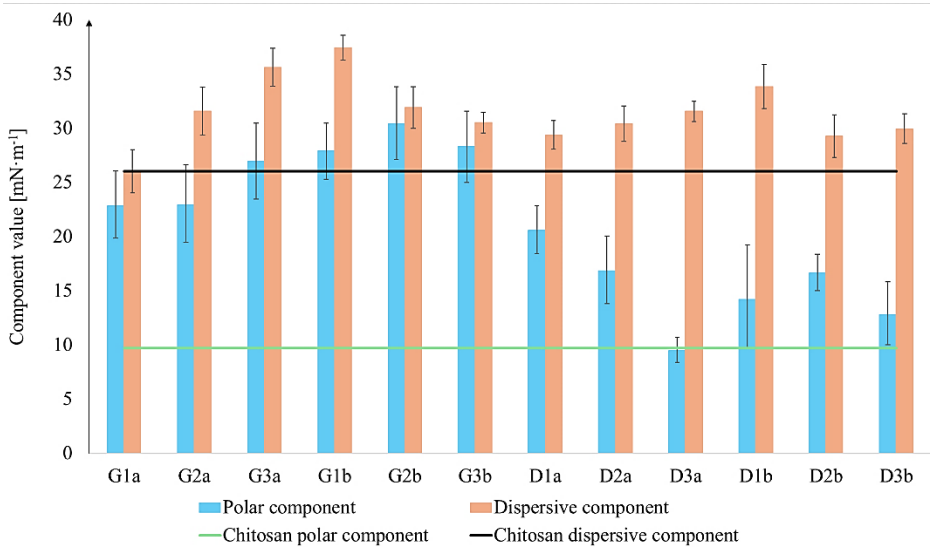

Figure 5. Free surface energy components of tested membranes.

The results obtained in this study are in agreement with literature findings for similar membranes [16, 18]. As no support layer was applied, the differences in thickness can be attributed solely to differences in drying times and variations in the membranes' internal

morphology (i.e., porosity). It was expected that tannic acid, as a strongly hydrophilic polyphenol, would decrease the water contact angle, but compared to the findings of Eteba *et al.* [16], there is no distinct effect. The increase of hydrophilicity in the G series is advantageous for water filtration, as it is connected to a lower tendency for fouling [22].

When the mechanical properties of the obtained membranes are analysed, the membranes' porous nature is of the most importance and must be taken into account. As parameters such as maximum tensile stress and Young's modulus depend on the cross-sectional area of the tested materials, they do not provide a complete picture for comparing materials with varying degrees of porosity. Thus, the line force density of the tested membranes (load per sample width, N/cm) was also included in the analysis, as the membranes were prepared using the same amounts of polymer and additives per unit surface area. As a result, all membranes should represent the same effective thickness. Actually, the G series membranes are thicker (0.40–0.84 mm) than the D series (0.26–0.42 mm). All mechanical parameters are collated in Table 2.

Table 2. Results of mechanical testing of the chitosan membranes.

Label	Elongation at break [%]	Line force density [N/cm]	Maximum tensile stress [MPa]	Young's modulus [MPa]
R	16.4 ± 3.9	2.9 ± 0.5	0.97 ± 0.19	6.0 ± 0.3
G1a	21.7 ± 3.8	1.3 ± 0.1	0.27 ± 0.01	1.3 ± 0.2
G1b	36.5 ± 13.7	1.8 ± 0.5	0.34 ± 0.11	1.4 ± 0.4
G2a	32.9 ± 5.1	1.9 ± 0.3	0.45 ± 0.07	1.8 ± 0.3
G2b	35.6 ± 5.8	1.9 ± 0.2	0.46 ± 0.04	2.0 ± 0.2
G3a	22.8 ± 7.2	1.8 ± 0.5	0.35 ± 0.11	0.9 ± 0.3
G3b	76.8 ± 18.6	2.3 ± 0.2	0.33 ± 0.07	0.6 ± 0.3
D1a	9.0 ± 0.4	1.9 ± 0.1	0.56 ± 0.03	5.2 ± 0.9
D1b	12.7 ± 5.6	1.9 ± 0.3	0.48 ± 0.12	3.0 ± 0.5
D2a	4.0 ± 2.9	1.2 ± 0.4	0.27 ± 0.14	4.2 ± 1.2
D2b	10.4 ± 0.4	1.8 ± 0.1	0.66 ± 0.07	6.0 ± 0.7
D3a	8.7 ± 2.0	2.0 ± 0.3	0.50 ± 0.09	4.8 ± 0.5
D3b	18.4 ± 1.2	3.0 ± 0.1	0.94 ± 0.06	6.2 ± 0.5

Results presented in Table 2 suggest that the addition of porogen disrupted the material structure, and the tannic acid used did not mitigate this phenomenon. Nonetheless, Young's moduli fall within the range between typical chitosan hydrogels and films [12].

3.2. Filtration Results

The microparticles used in this study are actual primary microplastics that have the potential of being a part of environmental samples. Utilising commercially available PVC, the obtained results are a step closer to environmental samples and are easily replicable.

Chitosan membranes are not widely used in filtration processes, as these membranes commonly exhibit low mechanical properties and poor water resistance, unless treated with a strong base. The main goal of this research was to assess the potential of chitosan membranes in microfiltration of PVC microplastics from water. At this early stage of research, the authors focused only on the chosen but important parameters, i.e., the cut-off point and filtration efficiency. The dead-end regime was employed for a simple and

controlled system to assess separation potential with rapid cake formation in mind. For the focus of this study, it was suitable and helped with ensuring a complete transfer of suspension through the membrane. However, in the future, the cross-flow regime should also be tested to assess the applicability of the obtained materials in this setup, long-term stability, fouling nature and scale-up potential. Suspension flux, averaged from the time required for the collection of the initial portion of suspension, varied within the range of 40–50 L/(m^2·h·bar) for G-series membranes, except G2a, and was approximately constant during the whole process. This suggests that fouling did not significantly affect the transport efficiency. In turn, all membranes from the D-series, except D3b, were non-permeable under applied experimental conditions. Moreover, all tested materials showed no visible damage when subjected to up to 2 bars of water pressure, although membranes D3b and G2a did not exhibit an increase in transmembrane pressure, suggesting that these membranes could be quickly disrupted at the start of the experiment.

Assuring complete transfer of the suspension through the PVDF membrane, it was possible to calculate the filtration efficiency of permeable membranes by extrapolating the number of particles observed on SEM images (Figure 6) and calculating the number of particles per 1 g of suspension. For the mass efficiency, it was assumed that all particles were spherical. The detailed results are presented in Figure 7 and summarised in Table 3. PVC was visually identified due to the high contrast of the microplastics deposited on the PVDF membrane.

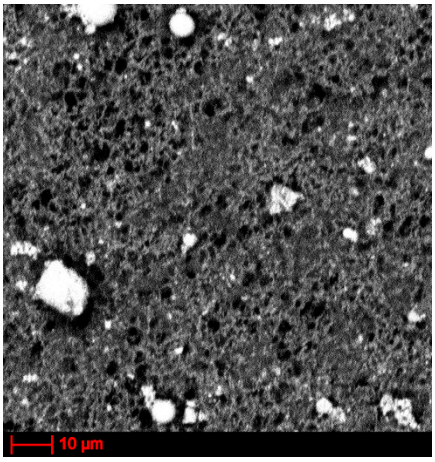

Figure 6. Exemplary SEM image of PVC microparticles collected during blank test.

Filtration efficiencies and particle size distributions in effluents indicate that membranes G2a and D3b were significantly worse than all other membranes, as expected from the water permeability results. The population of PVC particles over 4 µm in diameter was too small to be grouped into 0.1 µm classes and was therefore not shown in Figure 7. When grouped into 0.5 µm classes, the populations are sufficient enough to calculate the cut-off point of the prepared membranes. The remaining membranes exhibited very good filtration efficiencies, with over 90% of particles recovered. Despite the highest particle removal efficiency achieved by membrane G1b (99%), the high reproducibility of the G3 variant identifies it as the optimal composition among those evaluated.

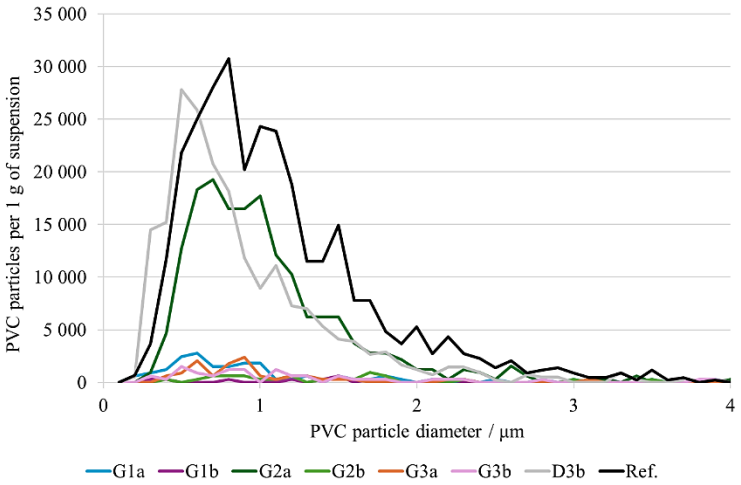

Figure 7. PVC particles size distribution in effluents from filtration experiments.

Table 3. Summary of the filtration experiment results.

Membrane	PVC particles per 1 g of suspension ×100	Numerical filtration efficiency [%]	Mass filtration efficiency [%]	Cut-off range [µm]
G1a	21.1	93.1	55.2	0.5–1
G1b	3.00	99.0	99.8	0–0.5
G2a	170	44.6	85.8	> 4
G2b	8.40	97.3	96.1	0–0.5
G3a	12.8	95.8	97.8	0–0.5
G3b	12.4	96.0	98.0	0–0.5
D3b	199	35.1	94.0	> 4
Reference	307	-	-	-

Compared to household multistage water filtration systems, the results are very promising [23]. Even though all systems tested by Altaee *et al.* [23] included a reverse osmosis membrane, fresh ones achieved efficiencies in the range 82–93%. The improved performance of the chitosan membranes produced can be attributed to the polymer's good adsorptive properties [11, 24]. Liu *et al.* [15] conducted a related study aimed at producing an ultrafiltration membrane from chitosan using the alkaline method for cross-flow filtration. In the separation of 1 µm polystyrene beads, these membranes exhibited 80–95% efficiency, while water permeance was in the range of 10–100 L/(m^2·h·bar). Both the literature and the procedures presented here for the production of porous chitosan-based membranes show great potential for the development of materials for microplastic separation.

4. Conclusions

Chitosan-based microfiltration membranes were successfully produced using simple, eco-friendly resources. The presented results show that chitosan can be utilised as

a material for filtration membranes, which, alongside adsorption applications, are a typical direction for research on this polymer. The neutralisation of chitosan citrate is a crucial step affecting the properties of the final membrane. The gelation of a highly viscous solution yields membranes suitable for microfiltration of PVC microplastics from water in dead-end filtration. The use of PEG and glucose as pore-forming agents induces formation of a highly hydrophilic surface, without worsening of the mechanical properties. Further studies on fouling and research on increasing permeability are needed to fully evaluate the potential of these membranes.

5. Author Contributions

Conceptualisation, M.C.; methodology, M.C., M.W., and D.P.; software, M.Sz. and P.R.; validation, M.W. and A.G.-G.; formal analysis, M.C. and M.W.; investigation, M.C., M.W., and D.P.; resources, M.Sz., P.R., and A.G.-G.; data curation, P.R. and A.G.-G.; writing—original draft preparation, M.C.; writing—review and editing, M.Sz. and A.G.-G.; visualisation, M.W.; supervision, P.R. and A.G.-G.; project administration, M.C. and A.G.-G. All authors have read and agreed to the published version of the manuscript.

6. References

[1] Ashokkumar V, Chandramughi VP, Mohanty K, Gummadi SN; (2025) Microplastic pollution: Critical analysis of global hotspots and their impact on health and ecosystems. Journal of Environmental Management 381, 124995. **DOI:** 10.1016/j.jenvman.2025.124995

[2] Conley K, Clum A, Deepe J, Lane H, Beckingham B; (2019) Wastewater treatment plants as a source of microplastics to an urban estuary: Removal efficiencies and loading per capita over one year. Water Research X 3, 100030. **DOI:** 10.1016/j.wroa.2019.100030

[3] Koonmee P, Vibhatabandhu P, Srithongouthai S; (2024) Microplastic contamination in landfill leachate and surface water: assessment of wastewater treatment efficiency at the nonthaburi waste management center, Thailand. South Eastern European Journal of Public Health 1451–1457. **DOI:** 10.70135/seejph.vi.2109

[4] Akarsu C, Kumbur H, Kideys AE; (2021) Removal of microplastics from wastewater through electrocoagulation-electroflotation and membrane filtration processes. Water Science and Technology 84(7), 1648–1662. **DOI:** 10.2166/wst.2021.356

[5] Pinto PE, Giacobbo A, Almeida GMD, Rodrigues MAS, Bernardes AM; (2025) Pressure-driven membrane processes for removing microplastics. Membranes 15(3), 81. **DOI:** 10.3390/membranes15030081

[6] Sarsour J, Ewert B, Janisch B, Stegmaier T, Gresser GT; (2025) Efficient filtration systems for microplastic elimination in wastewater. Microplastics 4(3), 36. **DOI:** 10.3390/microplastics4030036

[7] Pizzichetti ARP, Pablos C, Álvarez-Fernández C, Reynolds K, Stanley S, Marugán J; (2021) Evaluation of membranes performance for microplastic removal in a simple and low-cost filtration system. Case Studies in Chemical and Environmental Engineering 3, 100075. **DOI:** 10.1016/j.cscee.2020.100075

[8] Ding H, Zhang J, He H, Zhu Y, Dionysiou DD, Liu Z, Zhao C; (2021) Do membrane filtration systems in drinking water treatment plants release

nano/microplastics? Science of The Total Environment 755, 142658. **DOI:** 10.1016/j.scitotenv.2020.142658

[9] Commission Regulation (EU) 2023/2055 of 25 September 2023 amending Annex XVII to Regulation (EC) No 1907/2006 of the European Parliament and of the Council concerning the Registration, Evaluation, Authorisation and Restriction of Chemicals (REACH) as regards synthetic polymer microparticles (Text with EEA relevance); (2023).

[10] Hameed AZ, Raj SA, Kandasamy J, Baghdadi MA, Shahzad MA; (2022) Chitosan: A sustainable material for multifarious applications. Polymers 14(12), 2335. **DOI:** 10.3390/polym14122335

[11] Saheed IO, Oh WD, Suah FBM; (2021) Chitosan modifications for adsorption of pollutants – A review. Journal of Hazardous Materials 408, 124889. **DOI:** 10.1016/j.jhazmat.2020.124889

[12] Wahba MI; (2020) Enhancement of the mechanical properties of chitosan. Journal of Biomaterials Science, Polymer Edition 31(3), 350–375. **DOI:** 10.1080/09205063.2019.1692641

[13] Tu G, Li S, Han Y, Li Z, Liu J, Liu X, Li W; (2022) Fabrication of chitosan membranes via aqueous phase separation: Comparing the use of acidic and alkaline dope solutions. Journal of Membrane Science 646, 120256. **DOI:** 10.1016/j.memsci.2022.120256

[14] Zeng M, Fang Z; (2004) Preparation of sub-micrometer porous membrane from chitosan/polyethylene glycol semi-IPN. Journal of Membrane Science 245(1–2), 95–102. **DOI:** 10.1016/j.memsci.2004.08.004

[15] Liu X, Zou Z, Wang D, Du D, Li Z, Li W; (2024) Sustainable fabrication of chitosan membranes with optimized performance for ultrafiltration. Separation and Purification Technology 330, 125276. **DOI:** 10.1016/j.seppur.2023.125276

[16] Eteba A, Bassyouni M, Elzahar MH, El-shekhiby MZ; (2025) Development and optimization of biodegradable chitosan-based nanofiltration membranes for effective textile wastewater treatment. Separation and Purification Technology 367, 132852. **DOI:** 10.1016/j.seppur.2025.132852

[17] Bezerra MC, Duarte GA, Talabi SI, Lucas AA; (2022) Microstructure and properties of thermomechanically processed chitosan citrate-based materials. Carbohydrate Polymers 278, 118984. **DOI:** 10.1016/j.carbpol.2021.118984

[18] Cui Z, Beach ES, Anastas PT; (2011) Modification of chitosan films with environmentally benign reagents for increased water resistance. Green Chemistry Letters and Reviews 4(1), 35–40. **DOI:** 10.1080/17518253.2010.500621

[19] Cadogan EI, Lee C-H, Popuri SR, Lin H-Y; (2014) Effect of solvent on physico-chemical properties and antibacterial activity of chitosan membranes. International Journal of Polymeric Materials and Polymeric Biomaterials 63(14), 708–715. **DOI:** 10.1080/00914037.2013.867264

[20] Rubentheren V, Ward TA, Chee CY, Tang CK; (2015) Processing and analysis of chitosan nanocomposites reinforced with chitin whiskers and tannic acid as a crosslinker. Carbohydrate Polymers 115, 379–387. **DOI:** 10.1016/j.carbpol.2014.09.007

[21] Sionkowska A, Kaczmarek B, Lewandowska K; (2014) Characterisation of chitosan after cross-linking by tannic acid. Progress on Chemistry and Application of Chitin and its Derivatives 19(1), 135–138. **DOI:** 10.15259/PCACD.19.16

[22] Shahkaramipour N, Tran T, Ramanan S, Lin H; (2017) Membranes with surface-enhanced antifouling properties for water purification. Membranes 7(1), 13. **DOI:** 10.3390/membranes7010013

[23] Altaee RN, Al-Ahmady K, Mhemid RKS; (2024) Study the effectiveness of household water filtration systems in eliminating plastic particles in Mosul city, Iraq. Journal of Ecological Engineering 25(9), 24–33. **DOI:** 10.12911/22998993/190106

[24] Risch P, Adlhart C; (2021) A chitosan nanofiber sponge for oyster-inspired filtration of microplastics. ACS Applied Polymer Materials 3(9), 4685–4694. **DOI:** 10.1021/acsapm.1c00799

© Polish Chitin Society

Open Access: This article is distributed under the terms of the Creative Commons Attribution 4.0 International License (CC BY 4.0), which permits use, sharing, adaptation, distribution and reproduction in any medium or format, provided that appropriate credit is given to the original author(s) and source, a link to the license is provided, and any changes are indicated. Third-party material is included under the same license unless otherwise stated in a credit line.